5 April 1985, Volume 228, Number 4695 **SCIENCE**

The Sun and Nearby Stars: Microwave Observations at High Resolution

Mukul R. Kundu and Kenneth R. Lang

Microwave observations in the 1960's and 1970's added new dimensions to studies of solar active regions. The quiescent, or nonflaring, microwave emission at different wavelengths originates in levels of the solar atmosphere where the brightness temperatures (T_B) are comparable to the local electron temperatures. Values of T_B increase with increasing wavelength, λ, from $\sim 6.5 \times 10^3$ K at λ = 2 mm in the low chromosphere through $\sim 10^5$ K at λ = 2 cm in the chromosphere-corona transition region to $\sim 10^6$ K at λ = 20 cm in the low corona.

Summary. High-resolution microwave observations are providing new insights into the nature of active regions and eruptions on the sun and nearby stars. The strength, evolution, and structure of magnetic fields in coronal loops can be determined by multiple-wavelength observations with the Very Large Array. Flare models can be tested with Very Large Array snapshot maps, which have angular resolutions of better than 1 second of arc in time periods as short as 10 seconds. Magnetic changes that precede solar eruptions on time scales of tens of minutes involve primarily emerging coronal loops and the interactions of two or more loops. Magnetic reconnection at the interface of two closed loops may accelerate electrons and trigger the release of microwave energy in the coronal parts of the magnetic loops. Nearby main-sequence stars of late spectral type emit slowly varying microwave radiation and stellar microwave bursts that show striking similarities to those of the sun.

The microwave radiation of solar active regions is, with the exception of bursts, thermal in nature. The radiation at millimeter wavelengths is thermal bremsstrahlung. At centimeter wavelengths the gyroresonant radiation of thermal electrons accelerated by magnetic fields can compete with the bremsstrahlung of thermal electrons accelerated in the electric fields of ions. The dominant emission mechanism depends upon the wavelength and the physical conditions within the active region (*1*).

The solar active regions have intense magnetic fields that result in high degrees of circular polarization of the microwave emission. Magnetic fields permeate every level of the solar atmosphere above active regions. The microwave observations uniquely provide direct measurements of the strength and structure of the magnetic fields in the low corona and the transition region (between the photosphere and the corona). The observed radiation is circularly polarized in the extraordinary mode of wave propagation, with right-handed circular polarization corresponding to a positive magnetic field directed toward the observer. When thermal bremsstrahlung is the dominant radiation mechanism, the circular polarization is due to a propagation effect in the presence of a magnetic field. An electromagnetic wave passing through a magnetoionic medium is split into ordinary and extraordinary components, and the degree of circular polarization of the emergent radiation depends upon the optical depth for these two components. The longitudinal magnetic field strength (H_ℓ) can be inferred from the polarization and the optical depths. When gyroresonance dominates, the circularly polarized radiation is emitted at the second or third harmonic of the gyrofrequency. One is thus able to infer the magnetic field strength from the observed frequency (*2*).

The development of aperture synthesis instruments at radio wavelengths in the 1970's made possible the spatial resolution of the solar microwave sources and opened the way for comparisons with observations of similar angular resolution at optical and x-ray wavelengths. The high-resolution microwave observations were initially carried out at wavelength λ = 6 cm with the Westerbork Synthesis Radio Telescope in the Netherlands and the Very Large Array (VLA) spread out on a desert near Socorro, New Mexico. These observations indicated that gyromagnetic effects predominate in the regions above sunspots and that maps of circular polarization at 6 cm specify the structure of the coronal magnetic field (*3*). The high-resolution observations also indicated that the impulsive component of microwave bursts is usually located near the top of magnetic loops and that brightness and polarization changes precede solar bursts on time scales of tens of minutes (*4, 5*).

Three reviews, written when the solar application of microwave aperture synthesis was at an early stage, dealt almost solely with observations at 6 cm (*6*). This research area has matured in recent years, with multiple-wavelength VLA observations and snapshot synthesis maps produced in time periods as short as 10 seconds. We provide here a review of these recent developments. We begin with a discussion of the results of the multiple-wavelength studies that specify the three-dimensional structure of quies-

Mukul R. Kundu is professor and director of the Astronomy Program at the University of Maryland, College Park 20742. Kenneth R. Lang is an associate professor of astronomy at Tufts University, Medford, Massachusetts 02155.

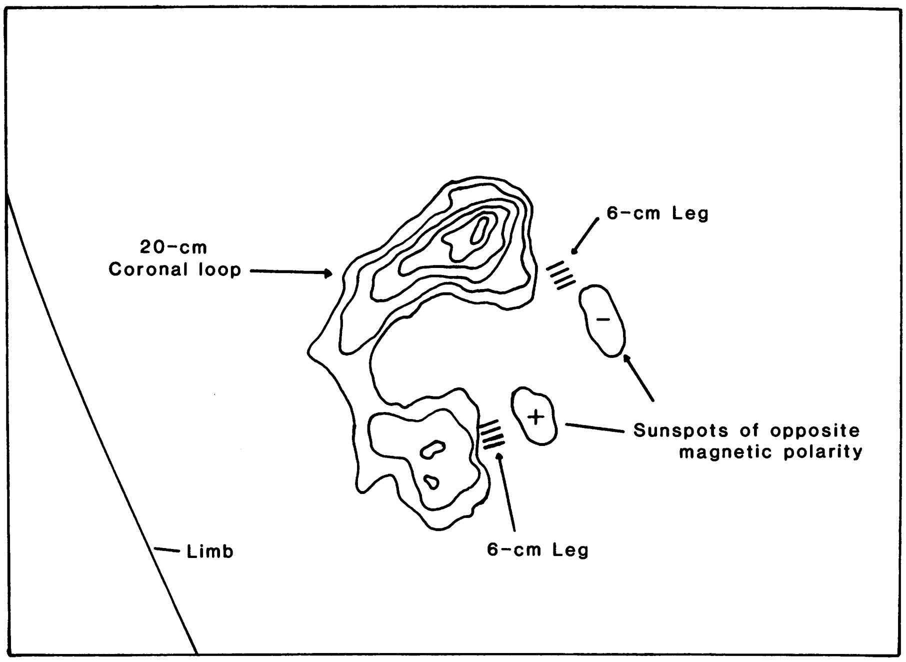

Fig. 1. Very Large Array synthesis map of a coronal loop at wavelength λ = 20 cm. The contours mark levels of equal T_B corresponding to 0.2, 0.4 . . . 1.0 times the maximum T_B of 2.0×10^6 K. A schematic portrayal of the 6-cm microwave emission, which comes from the legs of magnetic dipoles, is also shown, together with the underlying sunspots that are detected at optical wavelengths.

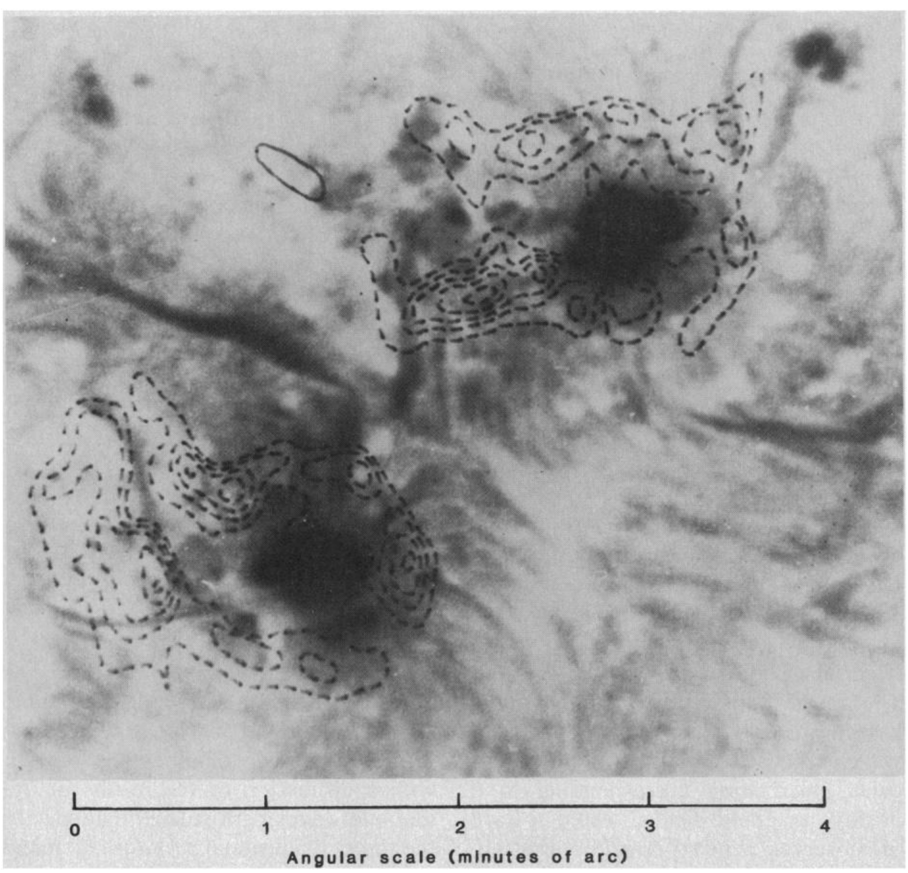

Fig. 2. A Westerbork Synthesis Radio Telescope synthesis map of circular polarization at λ = 6 cm overlaid on an Hα photograph obtained from the observatory at Athens. The contours are in steps of 1.5×10^5 K. The circularly polarized horseshoe structure that rings the sunspot umbra is due to gyroresonant emission in the curved magnetic fields of the sunspot penumbra. [Courtesy of *Astrophysical Journal (Letters)*]

cent, or nonflaring, active regions. Perhaps the most important new development has been the discovery of the microwave counterpart of the ubiquitous coronal loops, which heretofore have been observable only with satellite-borne x-ray telescopes.

Quiescent (Nonflaring) Microwave Emission from Solar Active Regions

Because the microwave emission from nonflaring active regions varies slowly over time scales of several hours, one may investigate its detailed structure by using the earth-rotation aperture synthesis technique (*7*). The instruments that one uses for this technique are generally composed of one or several linear arrays and utilize the rotation of the earth to change the relative orientation of the array and the radio source; Fourier inversion methods are used to determine the angular power distribution of a radio source from the array response (visibility functions). Synthesis maps of total intensity, *I*, describe the two-dimensional distribution of source brightness, whereas synthesis maps of circular polarization, or Stokes parameter *V*, describe the two-dimensional structure of the longitudinal magnetic field. Observations at different wavelengths sample different levels within the solar atmosphere, with longer wavelengths referring to higher levels. The heights of the microwave structures can be inferred from their angular displacements from underlying photospheric features, and the two-dimensional maps at different wavelengths in the microwave domain can be combined to specify the three-dimensional structure of solar active regions.

Multiple-wavelength synthesis observations of solar active regions have been carried out mainly at the VLA with λ = 2, 6, and 20 cm (*8*). The emission at these wavelengths often originates at different heights within the coronal loops that join sunspots of opposite magnetic polarity (Fig. 1). The 2-cm emission has been attributed to thermal bremsstrahlung of the 10^5 K plasma that overlies sunspots at heights h ~5,000 km where H_ℓ is ~10^3 G. Bright, highly polarized 6-cm cores mark the legs of dipolar loops with T_B ~2×10^6 to 5×10^6 K and h ~30,000 km above the underlying sunspots (Fig. 1). Values of H_ℓ of ~600 to 900 G are inferred from the fact that these cores emit gyroradiation at the second or third harmonic of the gyrofrequency. The 20-cm emission comes from the hot, dense plasma trapped within the magnetic loops that connect underlying sunspots. These coronal loops have $T_B = 2 \times 10^6$ to 4×10^6 K and extents of about 100,000 km. The 20-cm emission may be attributed to thermal bremsstrahlung or gyroresonant radiation, or both.

One of the most satisfying observational results has been the detection of circularly polarized ring-shaped or horseshoe structures predicted by the theory of gyroresonant emission from individual sunspots (*9*). Circular polarization maps at $\lambda = 6$ cm reveal highly polarized (up to 100 percent) structures that lie above the curved magnetic fields of sunspot penumbrae (see Fig. 2). There is no detectable circular polarization above the central sunspot umbrae where the magnetic fields project radially upward into the hot coronal regions. The total intensity of the 6-cm radiation is often enhanced above the sunspot umbrae, with $T_B \sim 10^6$ K; but it is also often enhanced above sunspot penumbrae and depressed over the umbrae. A 6-cm brightness depression above sunspot umbrae may be attributed to cool material above sunspot umbrae or to geometrical effects. For instance, there is negligible gyroresonant absorption when the angle between the magnetic field and the line of sight is small. Both cool material and variable absorption may be present, but the two effects cannot be easily disentangled.

Although gyroresonance in the legs of magnetic loops usually dominates the 6-cm emission, weaker bremsstrahlung can sometimes be detected at 6 cm near the loop apex. The coronal loops are more reliably mapped out if one uses the VLA at $\lambda = 20$ cm, where emission from the entire loop is routinely detected (*10*). The magnetic and temperature structure of coronal loops can be specified from the 20-cm observations. This emission is due to thermal gyroresonant absorption and/or bremsstrahlung of the same hot plasma that gives rise to x-ray emission by thermal bremsstrahlung. Because the magnetic energy density dominates the thermal energy density at coronal heights, this plasma remains trapped within the magnetic loops. Electron temperatures T_e of 2×10^6 to 4×10^6 K, electron densities N_e of 10^9 to 10^{10} cm^{-3}, loop extents of 10^9 to 10^{10} cm, and H_ℓ values of 200 G can be inferred from the 20-cm intensity and polarization maps. Thermal bremsstrahlung may also sometimes play a role in the 20-cm coronal loops, and in this case stronger magnetic fields of $H_\ell \sim 500$ G are inferred from the circular polarization if it is due to propagation effects.

Microwave Bursts from Solar Active Regions

The VLA has also recently been used to detect changes in the configuration of coronal magnetic fields and temperature enhancements within coronal loops that are important in the excitation of solar bursts. The origin and prediction of these powerful bursts is one of the most important and interesting problems of solar physics. It has long been known that solar eruptions are intimately connected with the magnetic fields in active regions, for the ultimate source of energy for these bursts must be magnetic ener-

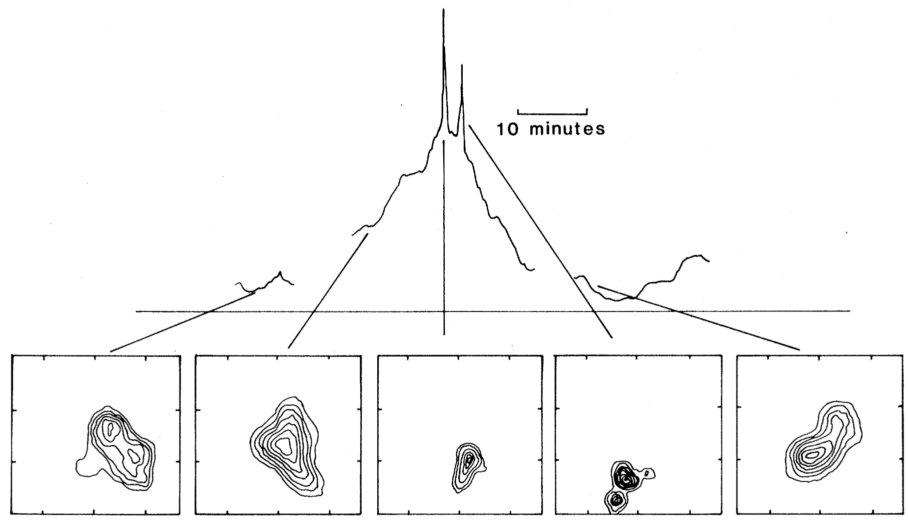

Fig. 3. The time profile of a solar burst at $\lambda = 20$ cm (top of figure) suggests heating within a coronal loop prior to the emission of two impulsive microwave bursts. The 20-cm VLA synthesis maps for 10-second intervals (bottom of figure) suggest that a coronal loop twisted in space. Energetic particles associated with hard x-ray emission at relatively low levels that occurred during the calibration gap shown in the figure may have either initiated the heating in the coronal loop or supplied it with microwave-emitting particles.

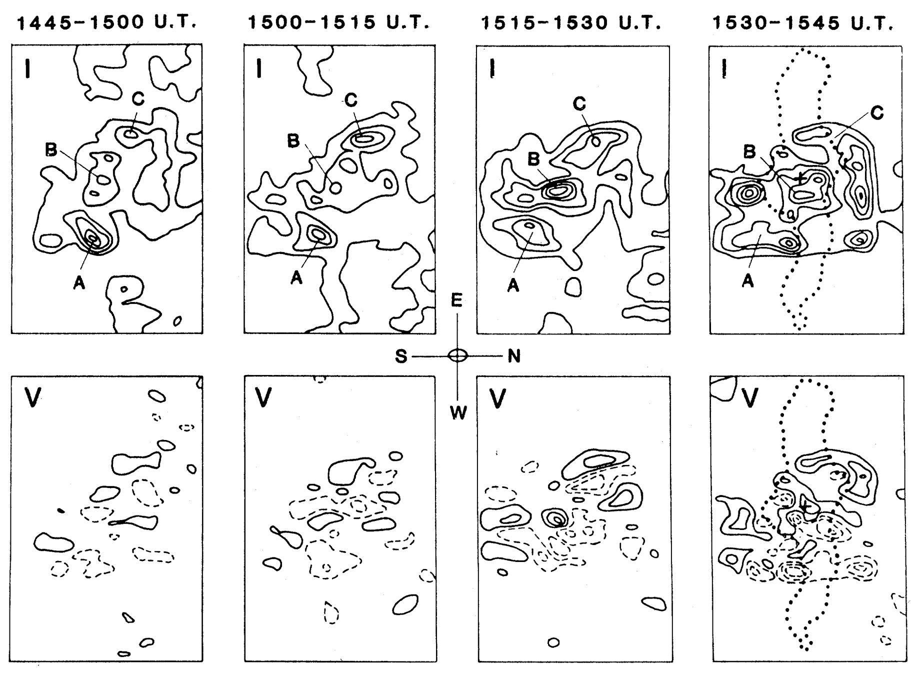

Fig. 4. Central 1′.1 × 1′.6 regions of preflare (15 minutes) maps of total intensity (*I*) and circular polarization (*V*) from $14^h\ 45^m$ to $15^h\ 45^m$ U.T. on 25 June 1980. The beam size is 4″ × 6″. The first contour is 1×10^6 K, and the contour interval is 2×10^6 K. Note the reversal of polarity in component B in the last map, close to the subsequent burst peak (marked by +). The dotted outline shows the extent of the burst source in the impulsive phase, $15^h\ 51^m$ to $16^h\ 00^m$ U.T. [Courtesy of *Astronomy and Astrophysics*]

gy. It has only recently been realized, however, that evolving magnetic fields in the solar corona may play a dominant role in triggering solar eruptions (*11*). Theoretical considerations indicate that loops emerging into the corona, magnetic shear within these loops, and interacting coronal loops can trigger solar bursts and supply their energy (*12*). One can now observe these effects for the first time by using the VLA to specify the magnetic field topology in active regions with angular resolutions of better than 1 second of arc in time periods as short as 10 seconds.

It has been known for several years that preflare changes in active regions are detected as increases in the intensity and polarization of the microwave emission at centimeter wavelengths. These increases precede solar eruptions on time scales of 10 minutes to an hour (*13*). They suggest that new magnetic loops are emerging or that existing magnetic fields are becoming more ordered. The high angular resolution provided by the VLA has now shown that these increases are related to preburst heating in coronal loops and to changes in the coronal magnetic field topology. The VLA snapshot maps have also made possible tests of flare models that could not be carried out at optical wavelengths.

The VLA results indicate that no single flare model is versatile enough to explain the diverse ways in which magnetic energy is dissipated in solar bursts. This is not terribly surprising in view of the magnetic complexity of solar active regions. Preburst changes can nevertheless be ordered into three major categories: (i) changes within a single coronal loop, (ii) the emergence of coronal loops, and (iii) interaction between coronal loops (*14*).

Single coronal loops or arcades of loops often begin to heat up and change structure about 15 minutes before the eruption of impulsive bursts. As illustrated in Fig. 3, heating within a magnetic loop was followed by impulsive microwave emission. Energetic particles associated with hard x-ray emission (high-energy x-ray photons) may have initiated or contributed to this heating. Radio and soft x-ray data have been combined to derive a peak T_e of 2.5×10^7 K and an average N_e of 10^{10} cm^{-3} during the heating phase of the example shown in Fig. 3. Future comparisons with observations at optical wavelengths may indicate whether the changing orientation of the microwave flaring region (Fig. 3) is related to the shear of photospheric magnetic fields, which is sometimes observed before a flare. Preburst heating and magnetic field changes can also occur in loops that are adjacent to, but spatially separated from, the sites of the impulsive bursts.

Preburst activity is also detected in coronal loops that are adjacent to those that emit bursts. New bipolar loops can emerge and interact with preexisting ones. When the polarity of the new emerging flux differs from that of the preexisting flux, current sheets are produced that trigger the emission of bursts.

An example of a reversal of polarization in a bipolar feature prior to the onset of a flare is shown in Fig. 4. It suggests either the emergence of new magnetic flux or a change in the topology of the magnetic field. Joint studies based on the use of Hα data and the ultraviolet spectrometer polarimeter aboard the Solar Maximum Mission Satellite led to the conclusion that rising and twisting of magnetic loops around the site of the flare triggered its onset (*15*).

Recent VLA solar observations may provide direct evidence of magnetic reconnection in microwave bursts (*16*). This is exemplified by a 6-cm burst, shown in Fig. 5, in which a gradual burst first appears with an east-west magnetic neutral line; superposed on it an intense emission extending along a new north-south neutral line appeared just before the impulsive burst occurred. This north-south line is indicative of the appearance of a new system of loops, possibly due to

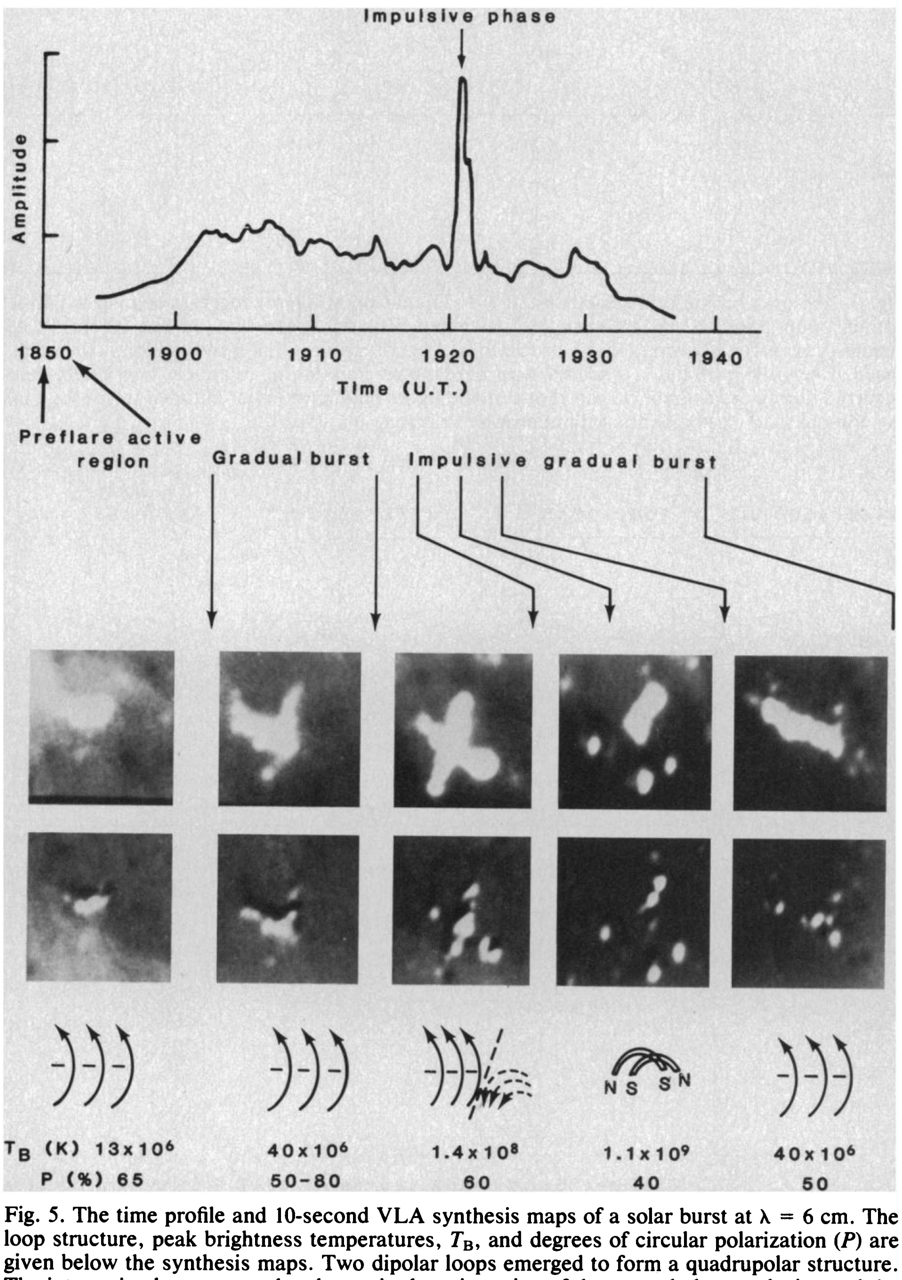

Fig. 5. The time profile and 10-second VLA synthesis maps of a solar burst at λ = 6 cm. The loop structure, peak brightness temperatures, T_B, and degrees of circular polarization (*P*) are given below the synthesis maps. Two dipolar loops emerged to form a quadrupolar structure. The interacting loops created a change in the orientation of the neutral plane and triggered the emission of an impulsive burst. [Courtesy of *Advances in Space Research*, Academic Press, New York]

reconnections. At the impulsive peak, the burst source structure changes and ultimately develops into two oppositely polarized bipolar regions or a quadrupole structure. A current sheet may have developed at the interface of two closed loops, thereby triggering the burst onset. The impulsive energy was probably due to magnetic reconnections of the field lines connecting the two oppositely polarized bipolar regions. It remains to be seen if the reconnection process can accelerate electrons to energies of the order of 100 keV or higher, which are responsible for microwave burst emission.

The microwave bursts are characterized by a strongly polarized, compact (5″ to 30″) impulsive component with a T_B of 10^7 to 10^9 K lasting between 1 and 5 minutes. This is followed by a larger, longer postburst component with relatively low polarization and T_B. The impulsive bursts are due to the gyrosynchrotron radiation of mildly relativistic electrons with energies of 100 to 500 keV.

The primary release of microwave energy takes place in the coronal part of magnetic loops. The impulsive part of the microwave energy is usually released in the upper parts of coronal loops and between the flaring Hα kernels (small regions) that mark the footpoints of magnetic loops (Fig. 6). The impulsive emitting region at $\lambda = 6$ cm occupies a large fraction of the flaring loops near their tops, whereas the 2-cm emission is more concentrated toward the loop apex. The microwave emission of the gradual phase that follows the impulsive burst at 2 cm is larger and is elongated along the magnetic field lines joining the Hα kernels.

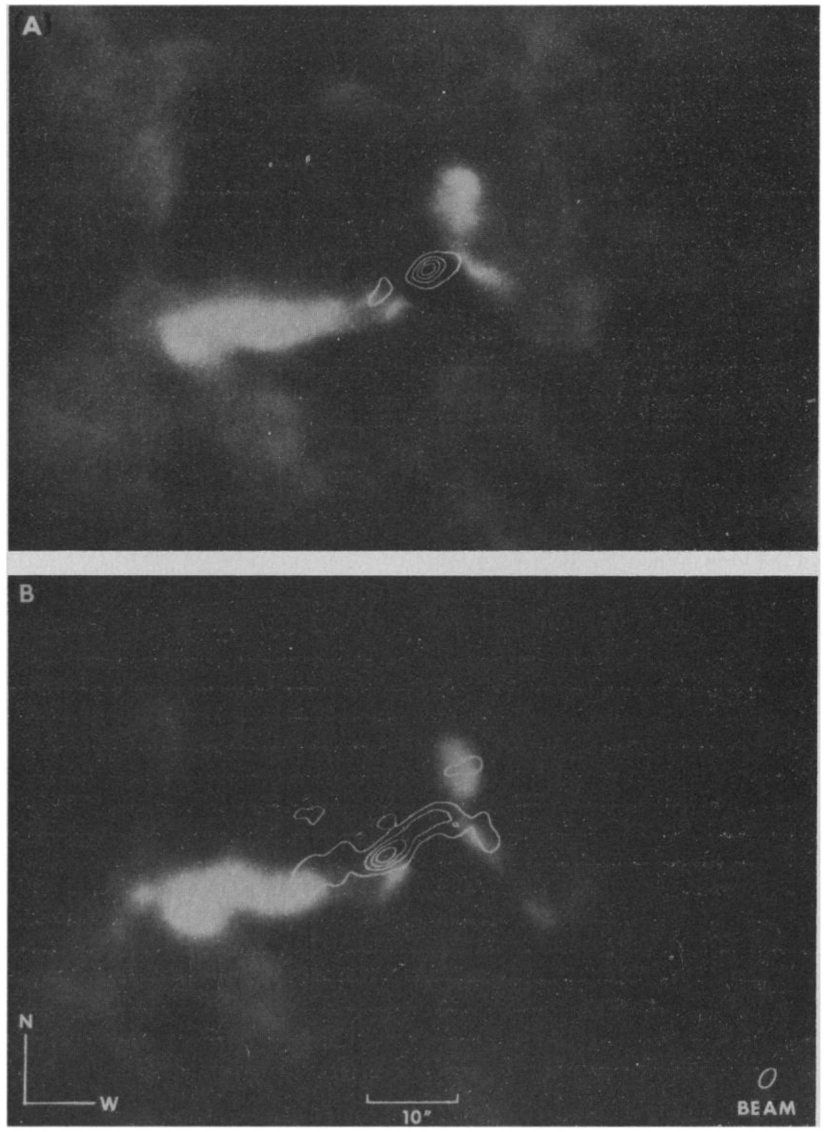

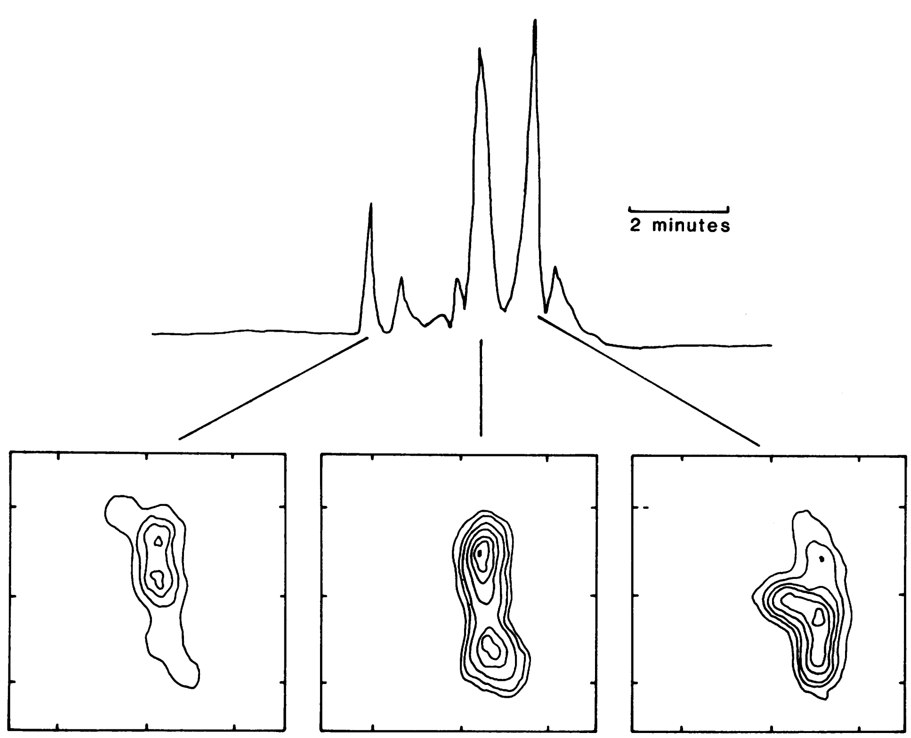

Fig. 6 (top). Very Large Array synthesis maps of the impulsive phase (A) and gradual phase (B) of a solar burst at $\lambda = 2$ cm (15.05 GHz) superimposed upon an Hα photograph of the flare taken at the same time at the Big Bear Solar Observatory, Big Bear, California. The microwave emission of the impulsive phase (peak $T_B = 2.5 \times 10^6$ K) was released at the top part of a dipolar loop, while the Hα kernels were emitted at the loop footpoints. The microwave emission of the gradual phase, which followed the impulsive phase and lasted for several minutes, is larger and is elongated along the magnetic field lines joining the Hα kernels (*22*). [Courtesy of *Astrophysical Journal (Letters)*] Fig. 7 (bottom). The time profile of successive impulsive bursts at $\lambda = 20$ cm (top) is compared with 10-second VLA synthesis maps at the same wavelength (bottom). Although the successive weak bursts were emitted from the same coronal loop, the successive intense bursts arose from spatially separated coronal loops having peak T_B values between 2×10^7 and 2×10^8 K. The contour intervals are in steps of 1.0×10^7 K.

The loop or arcade model of flares postulates the release of energy in the coronal part of a magnetic loop. This energy release [possibly through magnetic reconnection brought on by a tearing-mode instability (*12*)] impulsively heats the plasma in the upper part of the loop. A nonthermal tail of high-energy electrons (energies up to a few hundred kiloelectron volts) may also be produced at this time. The hot plasma is confined between a pair of conduction fronts which propagate down the legs of the loop with a velocity near the ion sound speed (*17*). Electrons with velocities greater than approximately three times the electron thermal speed in this region, however, are not confined by the conduction fronts and escape to the lower part of the loop. When the electron gyrofrequency exceeds the plasma frequency, the escaping electrons are unstable to the generation of electrostatic plasma waves which scatter the particles in pitch angle to a nearly isotropic distribution (*17*). This scattering can enhance the microwave emission from the upper part of the loop because more electrons are trapped in that part of the loop, and the scattered electrons have a higher mean pitch angle. Using an isotropic particle distribution and a uniform magnetic field, one can show (*12*) that microwave emission originates predominantly from the upper part of the loop and that a loop would appear larger in the optically thick regime than in the optically thin regime.

During the course of impulsive bursts, the microwave source sometimes drifts toward the limb. This apparent limbward motion can be attributed to a radial movement of expanding magnetic loops at velocities of a few hundred kilometers per second. Alternatively, bursts could be sequentially triggered at higher levels in the solar atmosphere.

There is also evidence for the sequential triggering of microwave bursts in different loops within magnetically complicated regions. As illustrated in Fig. 7, successive intense bursts can originate in adjacent coronal loops, whereas successive weaker bursts are located in the same coronal loop.

Microwave Emission from Nearby Stars of Late Spectral Type

Nearby main-sequence stars of late spectral type exhibit quiescent x-ray emission whose absolute luminosity may be as much as one hundred times that of the sun. These stars thus may have large-scale coronal loops and intense magnetic fields. The solar analogy indicates that the hot coronal plasma ought to be detected at $\lambda = 20$ cm and that polarized 6-cm emission should reveal the presence of large-scale magnetic structures.

In fact, the dwarf M flare stars exhibit slowly varying, circularly polarized microwave emission at $\lambda = 6$ cm that is analogous to the quiescent, or nonflaring, microwave emission from solar active regions (*18*). Brightness temperatures of 10^7 to 10^8 K are inferred if the microwave-emitting source covers the entire visible surface of the star. Brightness temperatures comparable to that of the sun's quiescent microwave emission ($T_B \sim 10^6$ K) are obtained if the stellar emitting region is three times as large as the visible star. The detected emission might then be explained as the gyroresonant emission from thermal electrons spiraling in magnetic fields with $H_\ell \sim 300$ G. Alternatively, the gyrosynchrotron emission of a small number of energetic electrons in starspots may account for the stellar microwave emission.

The dwarf M flare stars also exhibit microwave bursts that are similar to those emitted by the sun (*19*). For example, impulsive microwave bursts from the sun sometimes exhibit rapid millisecond fine structure that is 100 percent circularly polarized (*20*). Brightness temperatures as high as $\sim 10^{15}$ K have been inferred for the solar fine structure.

One impulsive burst from the dwarf M star AD Leo is composed of a rapid sequence of highly polarized (100 percent) spikes with rise times of less than 200 msec (Fig. 8). An upper limit to the linear size of the emitting region is 6×10^9 cm, the distance that light travels in 200 msec. If the emitting starspot is symmetric, it has an area that is less than 3 percent of the star's surface area, and its T_B exceeds 10^{13} K. The high T_B and high degrees of circular polarization of these star bursts can be explained in terms of electron-cyclotron maser emission at the second harmonic of the gyrofrequency in longitudinal magnetic fields of $H_\ell \sim 250$ G (*21*).

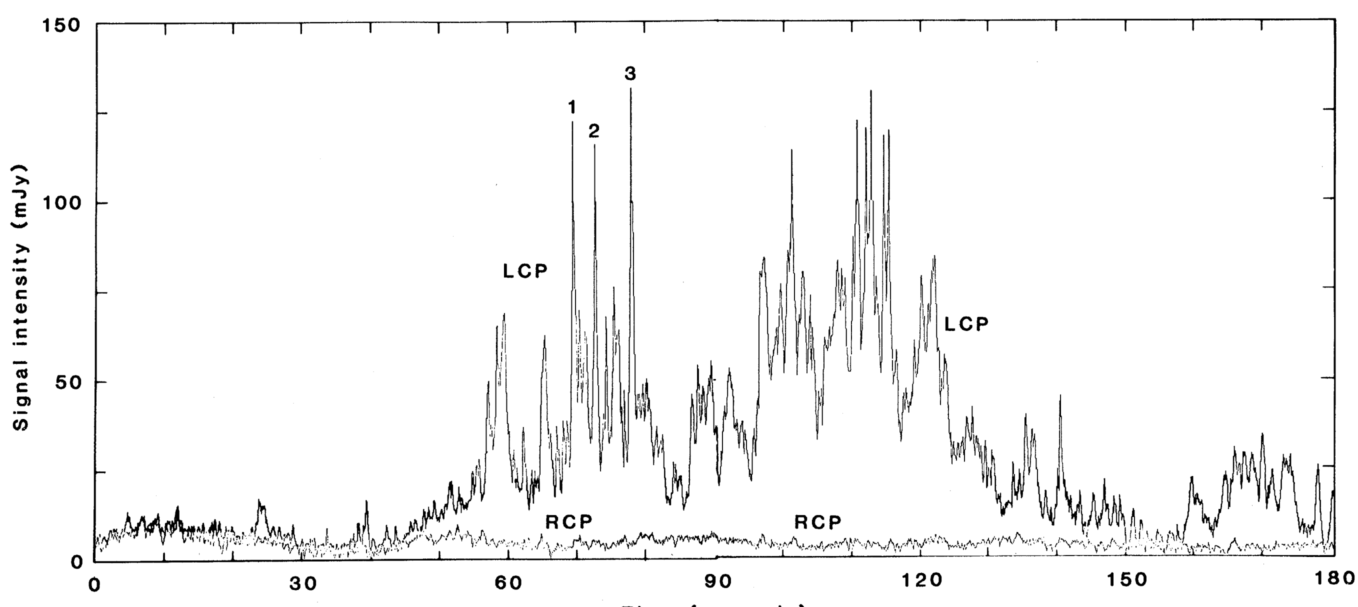

Fig. 8. Rapid, highly polarized spikes make up this 20-cm burst from the dwarf M star AD Leo. The spikes marked 1, 2, and 3 had rise times of less than 200 msec, indicating that the emitting source was less than 6×10^9 cm in diameter. Brightness temperatures in excess of 10^{13} K are infered for these spikes; LCP and RCP designate, respectively, left-handed and right-handed circularly polarized emission. [Courtesy of *Astrophysical Journal (Letters)*]

References and Notes

1. V. V. Zheleznyakov, *Sov. Astron. AJ* **6**, 3 (1962); T. Kakinuma and G. Swarup, *Astrophys. J.* **136**, 975 (1962); M. R. Kundu, *Solar Radio Astronomy* (Interscience, New York, 1965); P. Lantos, *Ann. Astrophys.* **31**, 101 (1968); E. Ya. Zlotnik, *Sov. Astron. AJ* **12**, 245 (1968); *ibid.*, p. 464; V. V. Zheleznyakov, *Radio Emission from the Sun and Planets* (Pergamon, New York, 1970); A. Kruger, *Introduction to Solar Radio Astronomy and Radio Physics* (Reidel, Boston, 1979).
2. J. A. Ratcliffe, *The Magneto-Ionic Theory* (Cambridge Univ. Press, Cambridge, 1962); K. R. Lang, *Astrophysical Formulae* (Springer, New York, 1974, 1980).
3. M. R. Kundu and C. E. Alissandrakis, *Nature (London)* **257**, 465 (1975); ______, J. D. Bregman, A. C. Hin, *Astrophys. J.* **213**, 278 (1977); K. R. Lang and R. F. Willson, *Nature (London)* **278**, 24 (1979); in *Radio Physics of the Sun* (International Astronomical Union Symposium 86), M. R. Kundu and T. E. Gergely, Eds. (Reidel, Dordrecht, 1980), p. 109; M. R. Kundu, E. J. Schmahl, M. Gerassimenko, *Astron. Astrophys.* **82**, 265 (1980); M. Felli, K. R. Lang, R. F. Willson, *Astrophys. J.* **247**, 325 (1981); R. Pallavacini, T. Sakurai, G. S. Vaiana, *Astron. Astrophys.* **98**, 316 (1981).
4. M. R. Kundu, T. Velusamy, R. H. Becker, *Sol. Phys.* **34**, 217 (1974); K. R. Lang, *ibid.* **36**, 351 (1974); C. E. Alissandrakis and M. R. Kundu, *Astrophys. J.* **222**, 342 (1978); M. R. Kundu, in *Radio Physics of the Sun* (International Astronomical Union Symposium 86), M. R. Kundu and T. E. Gergely, Eds. (Reidel, Dordrecht, 1980), p. 157; K. Marsh, G. J. Hurford, H. Zirin, *ibid.*, p. 191; K. R. Lang, R. F. Willson, M. Felli, *Astrophys. J.* **247**, 338 (1981).
5. K. A. Marsh and G. J. Hurford, *Astrophys. J.* **240**, L111 (1980).
6. ______, *Annu. Rev. Astron. Astrophys.* **20**, 497 (1982); M. R. Kundu, *Rep. Prog. Phys.* **45**, 1435 (1982); ______ and L. Vlahos, *Space Sci. Rev.* **32**, 405 (1982).
7. E. B. Fomalont, *Proc. Inst. Elec. Eng.* **61**, 1211 (1973).
8. K. R. Lang and R. F. Willson, in *Advances in Space Research—Proceedings of the 24th Meeting of COSPAR* (Pergamon, London, 1983), vol. 1, p. 91; ______, V. Gaizauskas, *Astrophys. J.* **267**, 455 (1983); R. K. Shevgaonkar and M. R. Kundu, *ibid.* **283**, 413 (1984).
9. G. B. Gel'freikh and B. I. Lubyshev, *Sov. Astron. AJ* **23**, 316 (1979); C. E. Alissandrakis, M. R. Kundu, P. Lantos, *Astron. Astrophys.* **82**, 30 (1980); C. E. Alissandrakis and M. R. Kundu, *Astrophys. J.* **253**, L49 (1982); K. R. Lang and R. F. Willson, *ibid.* **255**, L111 (1982).
10. M. R. Kundu and T. Velusamy, *Astrophys. J.* **240**, L63 (1980); T. Velusamy and M. R. Kundu, *ibid.* **243**, L103 (1981); K. R. Lang, R. F. Willson, J. Rayrole, *ibid.* **258**, 384 (1982); G. A. Dulk and D. E. Gary, *Astron. Astrophys.* **124**, 103 (1983); K. R. Lang and R. F. Willson, *ibid.* **127**, 135 (1983); D. McConnell and M. R. Kundu, *Astrophys. J.* **269**, 698 (1983).
11. D. Rust, *Sol. Phys.* **47**, 21 (1976); M. R. Kundu *et al.*, *Astron. Astrophys.* **108**, 188 (1982); R. F. Willson, *Sol. Phys.* **83**, 285 (1983); K. R. Lang and R. F. Willson, in *Advances in Space Research—Proceedings of the 24th Meeting of COSPAR* (Pergamon, London, 1983), vol. 2, p. 91; M. R. Kundu, *Proc. Int. Astron. Union Symp. 107* (1984), p. 185.
12. T. Gold and F. Hoyle, *Mon. Not. R. Astron. Soc.* **120**, 89 (1960); J. Heyvaerts, E. R. Priest, D. M. Rust, *Astrophys. J.* **216**, 123 (1977); D. S. Spicer, *Sol. Phys.* **53**, 305 (1977); S. I. Syrovatskii and V. D. Kuznetsov, in *Radio Physics of the Sun* (International Astronomical Union Symposium 86), M. R. Kundu and T. E. Gergely, Eds. (Reidel, Dordrecht, 1980), p. 445; V. D. Kuznetsov and S. I. Syrovatskii, *Sol. Phys.* **69**, 361 (1981); D. S. Spicer, *ibid.* **70**, 149 (1981); V. Petrosian, *Astrophys. J.* **255**, L85 (1982); B. V. Somov and S. I. Syrovatskii, *Sol. Phys.* **75**, 237 (1982); E. R. Priest, *ibid.* **86**, 33 (1983).
13. K. R. Lang, *Sol. Phys.* **52**, 63 (1977); M. R. Kundu, in *Radio Physics of the Sun* (International Astronomical Union Symposium 86), M. R. Kundu and T. E. Gergely, Eds. (Reidel, Dordrecht, 1980), p. 157; G. Hurford and H. Zirin, *Air Force Geophys. Lab. Rep. AFGL-TR-82-0017* (1982); R. K. Shevgaonkar and M. R. Kundu, *Astrophys. J.*, in press; K. R. Lang and R. F. Willson, *Advances in Space Research—Proceedings of the 25th Meeting of COSPAR* (Pergamon, London, in press).
14. M. R. Kundu, E. J. Schmahl, T. Velusamy, *Astrophys, J.* **253**, 963 (1982); ______, L. Vlahos, *Astron. Astrophys.* **108**, 188 (1982); T. Velusamy and M. R. Kundu, *Astrophys. J.* **258**, 388 (1982); M. R. Kundu, *Sol. Phys.* **86**, 205 (1983); M. R. Kundu, in *Advances in Space Research—Proceedings of the 24th Meeting of COSPAR* (Pergamon, London, 1983), vol. 1, p. 159; M. R. Kundu, D. M. Rust, M. Bobrowsky, *Astrophys. J.* **265**, 1084 (1983); R. F. Willson and K. R. Lang, *Astrophys. J.* **279**, 427 (1984); R. F. Willson, *Sol. Phys.* **92**, 189 (1984).
15. M. R. Kundu, V. Gaizauskas, B. Woodgate, E. J. Schmahl, R. Shine, H. Jones, *Astrophys. J. Suppl. Ser.*, in press.
16. M. R. Kundu, *Proc. Int. Astron. Union Symp. 107* (1984), p. 185.
17. J. C. Brown, D. B. Melrose, D. S. Spicer, *Astrophys. J.* **228**, 592 (1979); D. F. Smith and C. G. Lilliquist, *ibid.* **232**, 582 (1979); L. Vlahos and K. Papadopoulos, *ibid.* **233**, 717 (1979); G. D. Holman, M. R. Kundu, K. Papadopoulos, *ibid.* **257**, 354 (1984).
18. D. E. Gary and J. L. Linsky, *ibid.* **250**, 284 (1981); K. Topka and K. A. Marsh, *ibid.* **254**, 641 (1982); J. L. Linsky and D. E. Gary, *ibid.* **274**, 776 (1983).
19. D. E. Gary, J. L. Linsky, G. A. Dulk, *ibid.* **263**, L79 (1982); D. B. Melrose and G. A. Dulk, *ibid.* **259**, 844 (1982); K. R. Lang, J. Bookbinder, L. Golub, M. M. Davis, *ibid.* **272**, L15 (1983).
20. C. Slottje, *Nature (London)* **275**, 520 (1978); in *Radio Physics of the Sun* (International Astronomical Union Symposium 86), M. R. Kundu and T. E. Gergely, Eds. (Reidel, Dordrecht, 1980), p. 195; R. Zhao and S. Jin, *Sci. Sin. A* **25**, 422 (1982).
21. G. D. Holman, D. S. Eichler, M. R. Kundu, in *Radio Physics of the Sun* (International Astronomical Union Symposium 86), M. R. Kundu and T. E. Gergely, Eds. (Reidel, Dordrecht, 1980), p. 457; G. D. Holman, *Adv. Space Res.* **2**, 181 (1982); R. R. Sharma, L. Vlahos, K. Papadopoulos, *Astron. Astrophys.* **112**, 337 (1982); L. Vlahos, R. R. Sharma, K. Papadopoulos, *Astrophys. J.* **275**, 374 (1983).
22. Adapted from (*5*), plate 2.

23. This review would have been impossible without the fine contributions to solar radio astronomy made by R. F. Willson at Tufts University and C. E. Alissandrakis, E. J. Schmahl, T. Velusamy, and L. Vlahos while working for the University of Maryland. Radio astronomical studies of the sun and other active stars at Tufts University are supported under Air Force Office of Scientific Research grant AFOSR-83-0019-B. Investigations of flare stars at Tufts University are also supported by NASA grant NAG 5-477; whereas comparisons of VLA and Solar Maximum Mission satellite data are supported by NASA Guest Investigator grant NAG 5-501. Solar research in the Astronomy Program at the University of Maryland is supported under NSF grant ATM 84-15388, NASA grant NGR 21-002-199, and NASA contract NSG 5320. The Very Large Array is operated by Associated Universities Inc., under contract with the National Science Foundation.

Emotion and Facial Efference: A Theory Reclaimed

R. B. Zajonc

Nearly 80 years ago a book appeared in Paris under the title *Physionomie Humaine: Son Mécanisme et son Rôle Social* (*1*). The book, written by Israel Waynbaum, a physician, offered a radical theory of emotional expression, defying all previous ones, including Darwin's dominant theory. It clarified, for the first time, the function of emotional expression in the emotional process—the foremost problem in the study of emotions at the turn of the century. Yet Waynbaum's book received no attention and it has remained unknown until now. Neither the author nor his idea are to be found in the *Science Citation Index* or in numerous reviews of research on emotion or facial expression. In this article I review Waynbaum's theory, compare it with Darwin's, bring it up to date, and show that it forms a promising basis for a comprehensive theory of the emotions.

Waynbaum's analysis led him first to question the term "emotional *expression*." He feared that referring to facial movements as "expressions," the standard term since Aristotle, reinforced by Darwin's classic work (*2*), implicitly fixed their role in the emotional process, and "solved" the problem by definition. The term "expression" specifies a priori the causal sequence among emotional correlates, placing the efferent process at the terminus. As such, therefore, "expression" cannot be the cause of any other aspect of the emotional process. The term "expression" also implies the existence of an antecedent internal state which "expression" externalizes, manifests, and displays. It implies further that the antecedent internal state seeks externalization that forces itself onto the surface. Hence, there also exists the term "suppression." In many cases the behavioral output may well "express" an internal state, and some reactions are indeed suppressed. But it is by no means established that all facial gestures that are classified as expressions are caused by internal subjective states. It may be

The author is a professor of psychology at the University of Michigan, Ann Arbor 48104.